Non-Texture Inpainting by Curvature-Driven Diffusions (CDD)

Tony F. Chan and Jianhong Shen *

Department of Mathematics, UCLA
Los Angeles, CA 90095-1555
(*chan@math.ucla.edu*)

School of Mathematics & IMA
University of Minnesota
Minneapolis, MN 55455
(*jhshen@math.umn.edu*)

1 Introduction

Inpainting refers to the practice of artists of restoring ancient paintings. Simply speaking, inpainting is to complete a painting by filling in the missing information on prescribed domains. On such domains, the original painting has been damaged due to aging, scratching, or some other factors.

Inpainting and disocclusion in vision analysis are closely connected but also clearly different. Both try to recover the missing visual information from a given 2-D image, and mathematically, can be classified into the same category of inverse problems. The difference lies in both their goals and approaches.

The main goal of disocclusion is to model how human vision works to complete occluded objects in a given 2-D scene, and understand their physical orders in the direction perpendicular to the imaging plane, and thus reconstruct approximately a meaningful 3-dimensional world (Nitzberg, Mumford, and Shiota [14]). The outputs from disocclusion are complete objects, and their relative orders or depth. Inpainting, on the other hand, is to complete a 2-D image which have certain regions missing. The output is still a 2-D image. (In applications, a missing region can indeed be the 2-D projection of a real object, such as the female statue in Figure 9.) Therefore, from the vision point of view, inpainting is a lower level process compared to disocclusion.

This fundamental difference naturally influences the approaches. The main approach for disocclusion is to segment the regions in a 2-D image, and then

*Research supported by grants from NSF under grant number DMS-9626755 and from ONR under N00014-96-1-0277. Manuscript is available at the site of UCLA CAM Reports: *www.math.ucla.edu/applied/cam/index.html*.

logically connect those which belong to the projection of a same physical object, and finally generate the order or depth for all the completed objects. *Edge completion* is one crucial step during the whole process. Disocclusion also often uses some high level information about objects (such as the near symmetry of human faces). For inpainting, an ideal scheme should be able to reconstruct an incomplete 2-D image in every detail so that it looks "complete" and "natural." More specifically, *to inpaint, is not only to complete the broken edges, but also to connect each broken isophote (or level-line)*, so that the 2-D objects completed in such a way show their natural variation in intensity (or color for color images) [3, 6, 11].

This comparison helps us understand better the real nature of the inpainting problem in a broader context.

The terminology of *digital inpainting* was first introduced by Bertalmio, Sapiro, Caselles, and Ballester [3]. Inspired by the real inpainting process of artists, the authors invented a successful digital inpainting scheme (referred to below as *the BSCB inpainting scheme* for convenience) based on the PDE method. The authors also deepened the interest in digital inpainting by demonstrating its broad applications in text removal, restoring old photos, and creating special effects such as object disappearance from a scene.

Though a qualitative understanding based on the transportation mechanism can be well established, rigorous mathematical analysis on the BSCB scheme appears to be much more difficult. This has encouraged Chan and Shen [6] to develop a new inpainting model which is founded on the variational principle. Since the energy function is based on the total variational (TV) norm [6], the model is called *TV inpainting*. The TV inpainting scheme is surprisingly a close variation of the well known restoration model of Rudin, Osher and Fatemi [16, 17]. The Euler-Lagrange equation for the TV inpainting model is

$$\frac{\partial u}{\partial t} \text{ (or 0)} = \nabla \cdot \left[\frac{\nabla u}{|\nabla u|} \right] + \lambda_e (u - u^0), \tag{1}$$

valid on the entire image domain Ω. The extended Lagrange multiplier $\lambda_e = \lambda(1 - \chi_D)$, where χ_D is the characteristic function (or mask) of the inpainting domain D, and λ is as in the TV denoising scheme [16, 17]. Therefore, inside the inpainting domain, the model simply employs an anisotropic diffusion:

$$\frac{\partial u}{\partial t} \text{ (or 0)} = \nabla \cdot \left[\frac{\nabla u}{|\nabla u|} \right]. \tag{2}$$

The TV inpainting model also explains successfully some aspects of the human disocclusion process in vision psychology [6], including the *entanglement illusions* gathered and analyzed by Kanizsa, the great psychologist [6, 9].

The major drawback of the TV inpainting model is that it does not restore well a single object when its disconnected remaining parts are separated far apart by the inpainting domain (see Figure 1 for a typical example). Such dependency on the aspect ratio of the missing part of the object is against two facts:

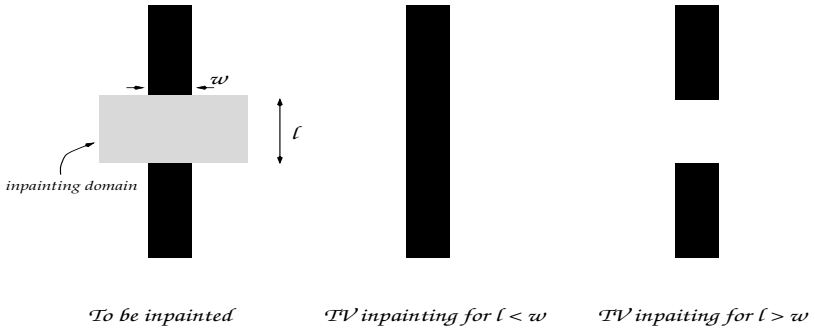

Figure 1: The output of the TV inpainting depends on the aspect ratio of the missing part of the object.

(a) The *Connectivity Principle* in the human disocclusion process. The vision psychology (Kanisza [9], Nitzberg, Mumford and Shiota [14]) shows that humans mostly seem to prefer the connected result. For example, in Figure 2, no matter what the relative ratio of w to l is, the whole bar always seems to be the best guess to most of us, psychologically.

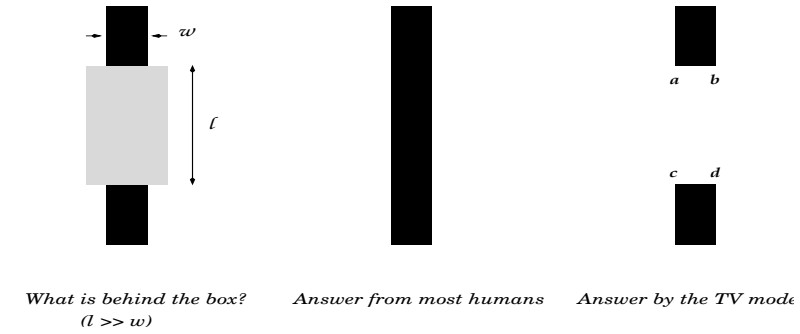

Figure 2: When $l > w$, the TV inpainting (or disocclusion) result is against the *Connectivity Principle* of human perception — humans mostly prefer having the two disjoint parts connected, even when they are far apart [9, 14].

(b) In application, an average image often contains objects of a large dynamic range of scales. Hence in most inpainting problems, it is commonly found that "slim" objects are broken by the inpainting domains even though the domains themselves are small (to humans). A good inpainting scheme should encourage the connection of these broken slim objects (lines, thin bars, or simple fiber-like textures; also see the numerical examples coming later).

In this paper, we propose a new inpainting model based on the diffusion mechanism as inspired by our previous work on the TV inpainting, aiming at

realizing the Connectivity Principle. Since in the new diffusion model, the conductivity coefficient depends on the curvature of the isophotes, we call such new diffusions *Curvature-Driven Diffusions* (CDD), as compared to the other diffusion models prevailing in image and vision analysis (Perona and Malik [15], Morel and Solomini [12]).

The CDD inpainting model, like the TV and BSCB models, is based on the PDE method. Therefore, generally it is directly applicable only to non-texture images, since visually meaningful statistical fluctuations in textures are often smoothed out by PDE's. For recent works related to texture inpaintings, see Wei and Levoy [18], and Igehy and Pereita [8]. In the future, we plan to apply the CDD inpainting scheme indirectly to texture images, based on the multiscale representation of textures (such as Burt and Adelson's Gaussian pyramid [4], and wavelets transforms).

The organization of the paper goes as follows. In Section 2, we explain what has been missed by the TV inpainting model, and why the CDD model can fix it. We formulate the CDD inpainting equations for both an ideal clean image, and for a more realistic noisy image. Connections to some related existing works in image and vision analysis are made. Section 3 addresses the numerical implementation of the CDD model. A discretization scheme based on finite differencing is explained. In Section 4, we show some typical applications of the CDD inpainting model in disocclusion, scratch removal, text removal, and special effects.

2 Inpainting via Curvature-Driven Diffusions (CDD)

We start out by first analyzing how the TV inpainting model can violate the Connectivity Principle. Then, based on such an analysis, we propose our CDD inpainting scheme.

In the TV model, the diffusion *strength* only depends on the *contrast* or *strength* of the isophotes, which is reflected in the expression for the conductivity coefficient: [1]

$$\hat{D} = \frac{1}{|\nabla u|}. \tag{3}$$

Therefore, the diffusion strength does not depend on the geometric information of an isophote. For a plane curve, its geometry is encoded into its scalar curvature κ.

Then why does this account for the TV's failure in completing a whole object for a large scale ratio $l : w$ as depicted in Figure 2? The rightmost one is the output from the TV inpainting, in which, the curvature $\kappa = \pm\infty$ at the four corners a, b, c and d. In contrast, in the"psychologically" correct output in the middle, all the isophotes are completed so that they stretch out as flatly as possible, or equivalently, the curvature κ is as small as possible (in magnitude).

[1] Since the symbol D is reserved in this paper for the inpainting domain to be consistent with the notations in [6], we shall use $\hat{D}$ instead for the conductivity coefficient to follow the conventional notation D.

The combination of the above qualitative analysis on what has gone wrong with the TV output when $l > w$, and what is characteristic with the psychologically correct output, inspires our CDD inpainting model, which we are now ready to introduce.

We modify the TV (or more generally, the Perona-Malik [15]) conductivity coefficient

$$\hat{D} = f(|\nabla u|), \tag{4}$$

to

$$\hat{D} = \frac{g(|\kappa|)}{|\nabla u|}, \tag{5}$$

where g is the "annihilator" of large curvatures and stabilizer of small curvatures:

$$g(s) = \begin{cases} 0, & s = 0 \\ \infty, & s = \infty \\ \text{in between}, & 0 < s < \infty. \end{cases} \tag{6}$$

With this choice, the diffusion gets stronger where the isophotes are having a larger curvature, while it dies away as the isophotes stretch out. Thus for the typical example shown in Figure 2, the CDD necessarily leads to a steady state that is closer to what most humans perceive in the middle. On the other hand, the steady state for the TV diffusion as plotted in the rightmost in Figure 2 is unstable in this new curvature-driven diffusion, since at the four corners a, b, c and d, the curvatures are $\pm\infty$ (or more precisely, behave like the Dirac delta functions locally along the edge isophotes). Such diffusion patterns are exactly what we have been expecting.

While the choice $g(\infty) = \infty$ has been thoroughly motivated above, the requirement of $g(0) = 0$ is less obvious. Suppose we allow $g(0) = a \neq 0$. Then the CDD model degenerates to the second order equation of TV inpainting for flatter isophotes. By doing so, we are again putting the Connectivity Principle in risk. Such speculation has been well supported by our numerical experiments.

In the current paper, we have chosen

$$g(s) = s^p, \quad s > 0,\ p \geq 1.$$

The curvature κ at a pixel $\mathbf{x}$ is the scalar curvature of the isophote through it, and is given by

$$\kappa = \nabla \cdot \left[\frac{\nabla u}{|\nabla u|} \right].$$

Thus, the CDD inpainting model reads

$$\begin{cases} \dfrac{\partial u}{\partial t} \text{ (or } 0) = \nabla \cdot \left[\dfrac{g(|\kappa|)}{|\nabla u|} \nabla u \right], & \mathbf{x} \in D \\ u = u^0, & \mathbf{x} \in D^c. \end{cases} \tag{7}$$

Here the inpaiting domain D is mathematically understood as an open set, i.e., not including its boundary; and u^0 is the available part of the image. If we solve

the time marching equation, then the initial condition can be any *compatible* guess, that is, any $u(\mathbf{x},0)$ that satisfies: $u(\mathbf{x},0)=u^0(\mathbf{x})$, $\mathbf{x}\in D^c$.

The *flux* field for the curvature-driven diffusion is

$$\mathbf{j}=-\hat{D}\nabla u=-\frac{g(|\kappa|)}{|\nabla u|}\nabla u, \tag{8}$$

which is anti-gradient and hence stable. Physically, we can treat the image function u as the density function of a certain species of particles. The available part of the original image u^0 acts as a constant source or sink of particles through the transactions at the boundaries. For example, suppose we are inpainting a broken bar in a uniform background. The connecting of the two broken parts is realized, in this particle diffusion picture, by the particles constantly fluxed into (or out of) the inpainting domain through its boundaries.

In most cases, the available part of the original image u^0 is noisy (such as in a digitally scanned photo due to the dust resting on the scanning glass). The CDD inpainting scheme formulated in Eq. (7) is sensitive to the noise since the latter will enter the inpainting domain via the boundary flux flow.

Two approaches can diminish this noise effect. First, one can denoise the available part of the original image *before* applying the CDD inpainting scheme. However, due to the topological complexity of a general inpainting domain, the implementation of most edge-enhancing denoising schemes is often nontrivial.

The second approach, is to intrinsically build the denoising action into the CDD inpainting scheme. Such practice seems to be natural for the human inpainting and disocclusion process. Humans seem to be the master in detecting features from the available portion of a noisy image, and at the same time, extending them into the inpainting domain.

Such methodology also appears in other mathematical models in image and vision analysis. The most famous one is the Mumford-Shah segmentation model [13], in which, segmentation and denoising are carried out simultaneously. Other examples include the Rudin-Osher-Fatemi [17] deblurring model, and our previous TV inpainting model [6].

This second approach suggests a model of a two-phase nature: inside the inpainting domain, we apply the CDD inpainting scheme (7); while outside, we activate the Rudin-Osher-Fatemi TV denoising model [16, 17]:

$$\frac{\partial u}{\partial t}\ (\text{or } 0)=\nabla\cdot\left[\frac{\nabla u}{|\nabla u|}\right]+\lambda(u-u^0),\qquad \text{for all}\ \ \mathbf{x}\in D^c. \tag{9}$$

The two actions can be concisely combined into one equation as in the TV inpainting scheme [6]:

$$\frac{\partial u}{\partial t}\ (\text{or } 0)=\nabla\cdot\left[\frac{G(\mathbf{x},|\kappa|)}{|\nabla u|}\nabla u\right]+\lambda_e(\mathbf{x})(u-u^0),\qquad \mathbf{x}\in\Omega. \tag{10}$$

Both the conductivity coefficient and Lagrange multiplier have two phases:

$$G(\mathbf{x},s)=\begin{cases}1, & \mathbf{x}\in D^c\\ g(s), & \mathbf{x}\in D,\end{cases}\qquad \lambda_e(\mathbf{x})=\begin{cases}\lambda, & \mathbf{x}\in D^c\\ 0, & \mathbf{x}\in D,\end{cases} \tag{11}$$

where g and λ come from Eq. (7) and the TV denoising model, separately. In applications, λ can be estimated from the noise level as discussed in the TV denoising model [6, 17]. In the two-phase equation (10), the phase transition occurs along the boundary of the inpainting domain. The boundary condition at $\partial\Omega$ for (10) is determined by the TV denoising equation, and thus a natural choice would be the Neumann adiabatic condition [7, 17].

The CDD inpainting model we propose here is closely related to some other existing works in image and vision analysis.

(a) Anisotropic diffusion has been a powerful tool in image and vision analysis. Well-known examples include the Perona-Malik diffusion for edge enhancement and detection [15]:

$$\frac{\partial u}{\partial t} = \nabla \cdot [f(|\nabla u|)\nabla u],$$

where $f(s)$ is a non-negative function representing the conductivity coefficient inversely proportional to the strength of an isophote; and its generalization in the framework of mean curvature motions by Alvarez, Lions and Morel [1]:

$$\frac{\partial u}{\partial t} = f(\nabla G_\sigma * u)\, |\nabla u|\, \nabla \cdot \left[\frac{\nabla u}{|\nabla u|}\right], \tag{12}$$

where G_σ is a Gaussian mollifier with the filtering scale σ, and $f(s)$ is a "time-corrector." The nonlinear diffusion operator is also important in Nitzberg, Mumford and Shiota's work in modeling disocclusion and depth [14]. The recent monograph by Weickert [19] is completely devoted to the topic of diffusion in image analysis.

All these diffusion models are of second-order and the diffusion depends solely on the strength of an isophote, but not on its geometry, i.e., the curvature. In Alvarez-Lions-Morel's formula (12), although the curvature appears, its action is on the propagation speed along the normal characteristics, not on the diffusion. The CDD is of third-order, and both the strength and geometry of isophotes determine the diffusion. To our best knowledge, such diffusion model is introduced in this paper for the first time in image analysis.

(b) The main part of the BSCB inpainting scheme [3] is also a third order equation:

$$\frac{\partial u}{\partial t} = \nabla^\perp u \cdot \nabla L(u),$$

where, $\nabla^\perp u$ is the 90-degree-rotated copy of the gradient, and $L(u)$ is an operator that evaluates the degree of smoothness. For example, the authors mainly used $L(u) = \Delta u$, the Laplacian. It is very interesting to note the completely "orthogonal" manners of BSCB's equation and our CDD: the BSCB equation is based on the elegant intuition of transportation (or propagation) of smoothness along the isophotes, while the CDD diffuses image

pixel information *perpendicular* to isophotes (i.e., along the normal directions). It will be interesting to explore the possibility of combining these two complementary models.

(c) We would also like to mention some other interesting works on non-texture inpaintings or disocclusions, which take different approaches. Caselles, Morel and Sbert in [5] developed the axiomatic framework for local image interpolations based on second order differential operators. Masnou and Morel in [11] proposed the functionalization of the 1-dimensional *Euler's Elastica* [14] as a variational formulation for non-texture disocclusion problems. The authors solved it numerically by matching and connecting individual broken isophotes using dynamical programming. In their work on nonlinear image interpolation, Armstrong, Kokaram and Rayner [2] proposed to use the min-max function as the predictor for missing image information, and formulated a least-square error minimization problem. Numerically, it was solved using a combination of simulated annealing and the conjugate gradient method. It is apparent from these examples, that generally the inpainting problem is very ill-posed, and fast numerical implementation is as challenging as coming up with a right mathematical model for inpaintings.

Since our CDD inpainting model is based on PDE's, its implementation naturally depends on the numerical PDE method.

3 Numerical Implementation

In this section, we explain the explicit time marching scheme for our CDD inpainting model (7) or (10). Take (7) for example:

$$\frac{\partial u}{\partial t} = -\nabla \cdot \mathbf{j}.$$

The explicit scheme iterates as:

$$u^{(n+1)} = u^{(n)} - \Delta t \, \nabla \cdot \mathbf{j}^{(n)},$$

where Δt is the numerical time step, and (n) denotes the sampling at $n\Delta t$. We now detail on the spatial discretization.

The CDD inpainting equation (7) or (10) is of 3rd order and in the divergence form. On the natural rectangular pixel grid of a given image, we take the half-point central difference for the divergence operator. That is, near a pixel, say $(0,0)$ (see Figure 3), the divergence form $\nabla \cdot \mathbf{j}$ is discretized to (assuming that $\mathbf{j} = (\mathbf{j}^1, \mathbf{j}^2)$)

$$\frac{\mathbf{j}^1_{(\frac{1}{2},0)} - \mathbf{j}^1_{(-\frac{1}{2},0)}}{h} + \frac{\mathbf{j}^2_{(0,\frac{1}{2})} - \mathbf{j}^2_{(0,-\frac{1}{2})}}{h}.$$

Here the CDD flux $\mathbf{j}$ is given by the expression (8), according to which, we need to obtain the half-point values

$$\nabla u_{(i,j)}, \qquad \kappa_{(i,j)}, \qquad ij = 0, \;\; |i| + |j| = \frac{1}{2}.$$

Take $(i, j) = (\frac{1}{2}, 0)$ for example (refer to Figure 3):

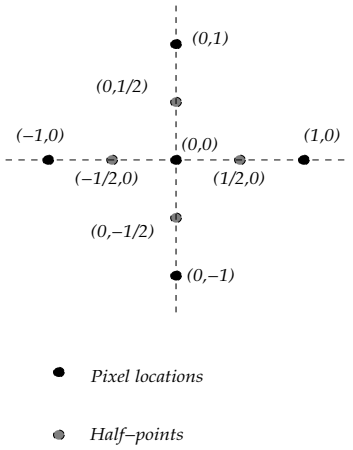

Figure 3: Numerical implementation.

(I) The expression for $\nabla u_{(\frac{1}{2},0)}$.

We have

$$\nabla u_{(\frac{1}{2},0)} = \left(\frac{\partial u}{\partial x}\bigg|_{(\frac{1}{2},0)}, \; \frac{\partial u}{\partial y}\bigg|_{(\frac{1}{2},0)} \right) \simeq \left(\frac{u_{(1,0)} - u_{(0,0)}}{h}, \; \frac{u_{(\frac{1}{2},1)} - u_{(\frac{1}{2},-1)}}{2h} \right).$$

For the new half-point values $u_{(\frac{1}{2},\pm 1)}$, we take the average of $u(0, \pm 1)$ and $u(1, \pm 1)$. Then both the $\nabla u_{(\frac{1}{2},0)}$ and $|\nabla u|_{(\frac{1}{2},0)}$ are represented by the pixel values.

(II) The expression for $\kappa_{(\frac{1}{2},0)}$.

Recall that

$$\kappa = \nabla \cdot \left[\frac{\nabla u}{|\nabla u|} \right] = \frac{\partial}{\partial x} \left[\frac{u_x}{|\nabla u|} \right] + \frac{\partial}{\partial y} \left[\frac{u_y}{|\nabla u|} \right].$$

Thus, we can use again the central difference divergence form for the half-point value $\kappa_{(\frac{1}{2},0)}$. For example,

$$h \cdot \frac{\partial}{\partial x} \left[\frac{u_x}{|\nabla u|} \right]_{(\frac{1}{2},0)} \simeq \left[\frac{u_x}{|\nabla u|} \right]_{(1,0)} - \left[\frac{u_x}{|\nabla u|} \right]_{(0,0)}.$$

For the new quantities like $(u_x/|\nabla u|)_{(1,0)}$, we then simply use the ordinary pixel wise central difference. In this way, the half-point curvature $\kappa_{(\frac{1}{2},0)}$ is expressed by the image pixel values.

Since we are always using the divergence form, certain conservation-law like results can be established, and, the numerical scheme is indeed stable according to our experiments.

Since the numerical scheme only utilizes central differencing, it is invariant under *digital rotations* of the input image, namely, multiples of $\pi/2$. (Under digital rotations, the image data always live on a rectangular grid.)

As the time steps increase, the numerical image function u stably converges to the final result. However, such time marching is generally slow for images of large size. Thus, acceleration techniques are worthwhile to investigate. For example, one can imitate the Marquina-Osher speeding modification for the TV diffusion [10].

One simple technique that we have used is to start the CDD time marching with a good initial guess $u(\mathbf{x}, 0)$: we run the TV inpainting model (1) first, and its output is then fed into the CDD scheme as a good initial guess. Since the TV inpainting model is of second order, and allows a positive energy functional [6], the time marching step can be much larger than the 3rd order CDD, and the output converges much faster. Besides the time marching approach for the TV inpainting model, Chan and Shen in [6] also solved directly its steady state equation via the linearization and relaxation techniques in numerical mathematics.

4 Examples of CDD Inpainting

In this section, we show some typical numerical examples and applications of the CDD inpainting scheme, which include simple disocclusions, restoration of an old photo with scratches, text removal from an image, and the special effect of removing an object from a scene (as inspired by [3]). The individual captions give more detailed explanations. Unless notified, the annihilator of large curvatures in Eq. (6) is set to be $g(s) = s$. (Our numerical experiments do not show significant difference among the different choices of $g(s) = s^p$ with distinct p values.)

Acknowledgments

The authors would like to thank G. Sapiro's group at ECE, University of Minnesota, for introducing us this interesting problem, and for generously exposing their new work and ideas to us. The authors would also like to thank Stan Osher, Luminita Vese, Sung Ha Kang, and Laurent Demanet for their support and help.

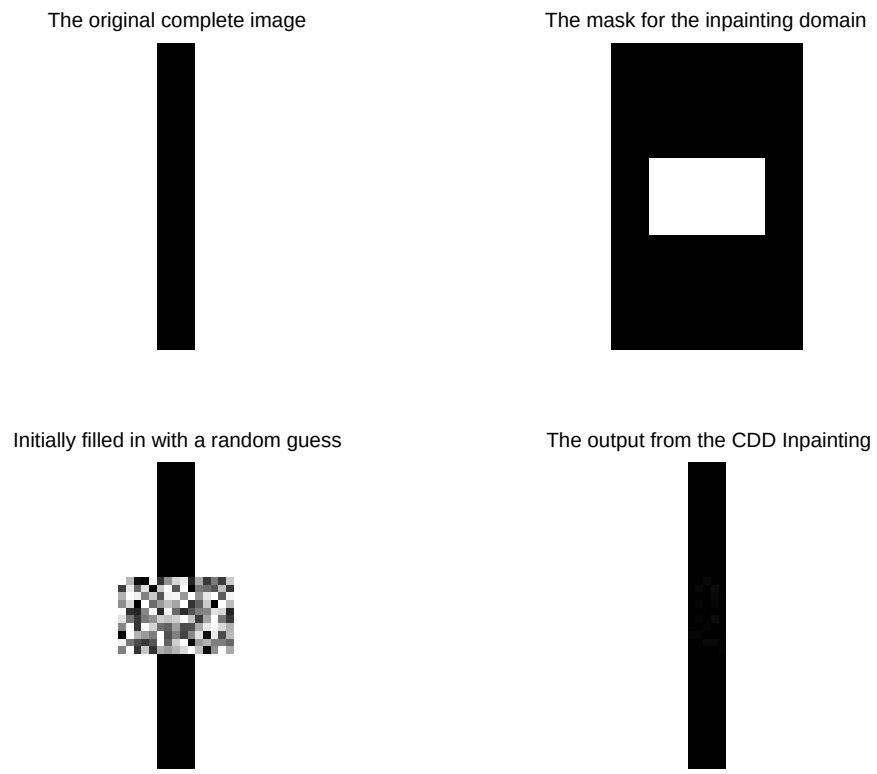

Figure 4: Inpainting a broken bar. Here the inpainting scale l is much larger than the width w of the bar. Therefore, the TV inpainting model [6] will output two separated bars. The CDD inpainting produces a whole bar, which is what most humans tend to perceive.

References

[1] L. Alvarez, P.-L. Lions, and J.M. Morel. Image selective smoothing and edge detection by nonlinear diffusion (II). *SIAM J. Num. Anal.*, 29:845–866, 1992.

[2] S. Armstrong, A. Kokaram, and P.J.W. Rayner. Nonlinear interpolation of missing data using min-max functions. *IEEE Int. Conf. Nonlinear Signal and Image Processings*, 1997.

[3] M. Bertalmio, G. Sapiro, V. Caselles, and C. Ballester. Image inpainting. Technical report, ECE-University of Minnesota, 1999.

[4] P. Burt and E. Adelson. The Laplacian pyramid as a compact image code. *IEEE Trans. Comm.*, 31:482–540, 1983.

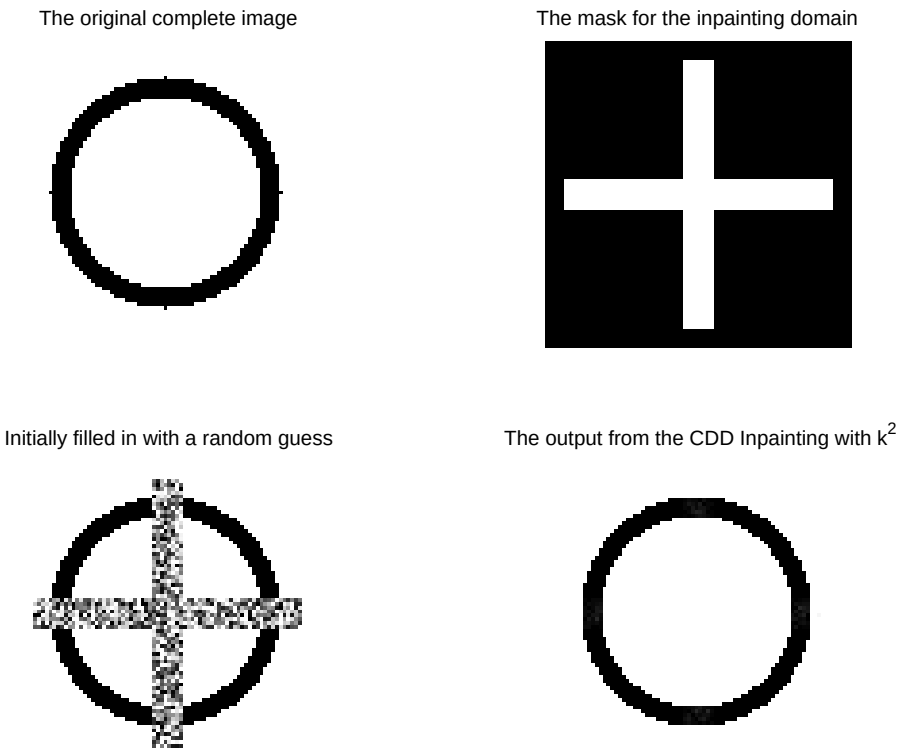

Figure 5: Inpainting a broken ring. Certainly, this example can also be understood as a thick cross occluding a thin ring. Again the TV inpainting model outputs four disconnected arcs, while the CDD inpainting scheme successfully completes the ring to the first order (i.e. using straight lines for circular arcs).

[5] V. Caselles, J.-M. Morel, and C. Sbert. An axiomatic approach to image interpolation. *IEEE Trans. Image Processing*, 7(3):376–386, 1998.

[6] T. Chan and J. Shen. Mathematical models for local deterministic inpaintings. Submitted. UCLA CAM Report 00-11 available at: *www.math.ucla.edu/applied/cam/index.html*, 2000.

[7] T. Chan and J. Shen. Variational restoration of non-flat image features: models and algorithms. *SIAM J. Appl. Math.*, in press, 2000.

[8] H. Igehy and L. Pereira. Image replacement through texture synthesis. *Proceedings of 1997 IEEE Int. Conf. Image Processing.*

[9] G. Kanizsa. *Organization in Vision.* Praeger, New York, 1979.

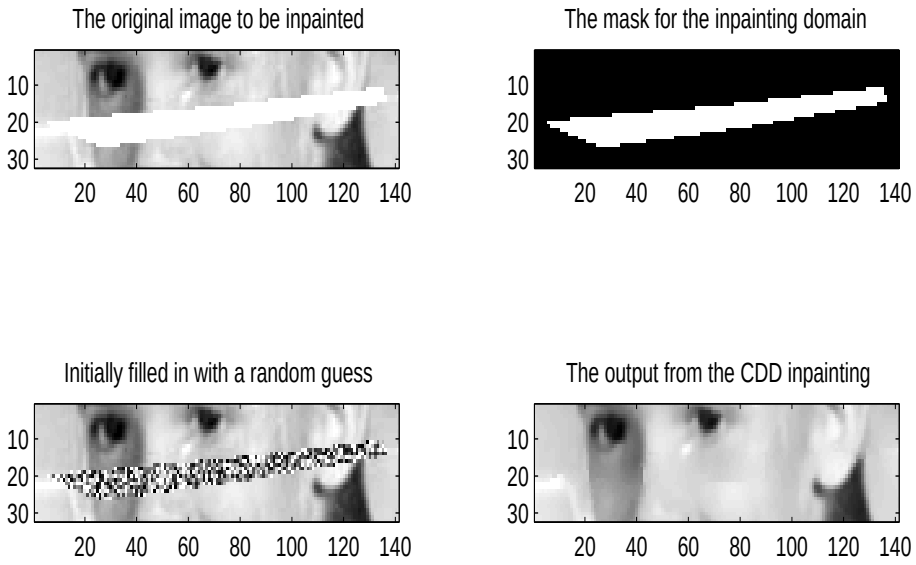

Figure 6: Removing scratches in a damaged photograph. From this example, one sees the difference between inpainting and disocclusion. In vision research, disocclusion mostly deals with boundary edges, while for inpainting, we have to complete isophotes (i.e. level lines) in all kinds of contrast, including weak edges such as the shaded side of the nose in the present image. (Image source: [3].)

[10] A. Marquina and S. Osher. *Lecture Notes in Computer Science*, volume 1682, chapter "A new time dependent model based on level set motion for nonlinear deblurring and noise removal", pages 429–434. 1999.

[11] S. Masnou and J.-M. Morel. Level-lines based disocclusion. *Proceedings of 5th IEEE Int'l Conf. on Image Process., Chicago*, 3:259–263, 1998.

[12] J.-M. Morel and S. Solimini. *Variational Methods in Image Segmentation*, volume 14 of *Progress in Nonlinear Differential Equations and Their Applications*. Birkhäuser, Boston, 1995.

[13] D. Mumford and J. Shah. Optimal approximations by piecewise smooth functions and associated variational problems. *Comm. Pure Applied. Math.*, XLII:577–685, 1989.

[14] M. Nitzberg, D. Mumford, and T. Shiota. *Filtering, Segmentation, and Depth*. Lecture Notes in Comp. Sci., Vol. 662. Springer-Verlag, Berlin, 1993.

[15] P. Perona and J. Malik. Scale-space and edge detection using anisotropic diffusion. *IEEE Trans. Pattern Anal. Machine Intell.*, 12:629–639, 1990.

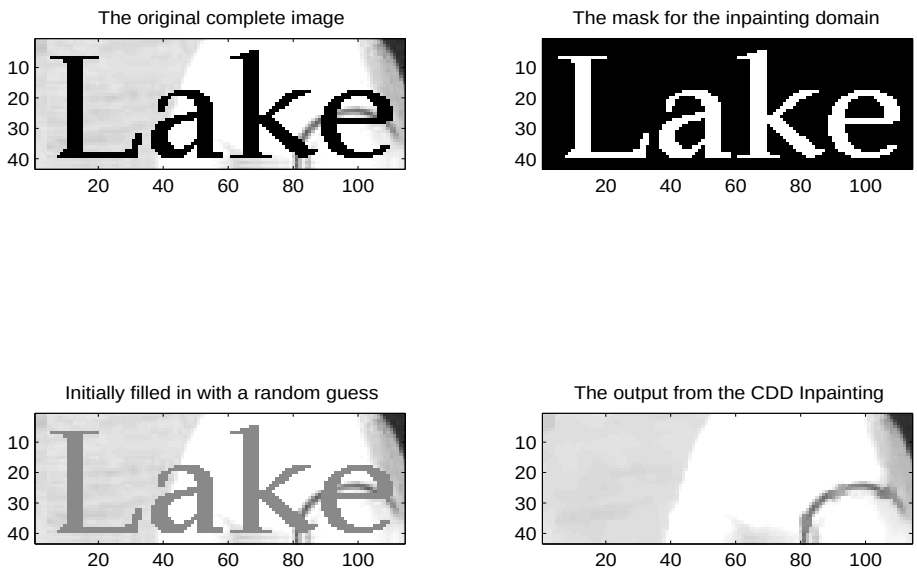

Figure 7: Removing thick text from an image. This example partially shows why in most inpainting applications, thin lines or bars should be connected. If we had used the TV inpainting model [6], the single black rim of the T-shirt (around the arm) would have been broken since its width is smaller than that of the letters at the intersections.

[16] L. Rudin and S. Osher. Total variation based image restoration with free local constraints. *Proc. 1st IEEE ICIP*, 1:31–35, 1994.

[17] L. Rudin, S. Osher, and E. Fatemi. Nonlinear total variation based noise removal algorithms. *Physica D*, 60:259–268, 1992.

[18] L.-Y. Wei and M. Levoy. Fast texture synthesis using tree-structured vector quantization. Preprint, Computer Science, Stanford University, 2000; Also in *Proceedings of SIGGRAPH 2000.*

[19] J. Weickert. *Anisotropic Diffusion in Image Processing.* Teubner-Verlag, Stuttgart, Germany, 1998.

The image to be inpainted

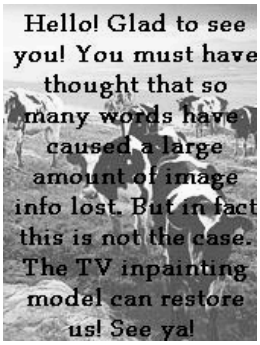

The inpainting domain is the text region

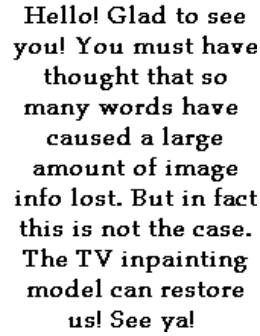

After inpainting

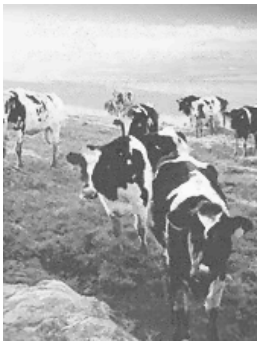

Figure 8: Removal of dense text. One major advantage of PDE models such as the CDD here is that it allows the inpainting domain to have any topology.

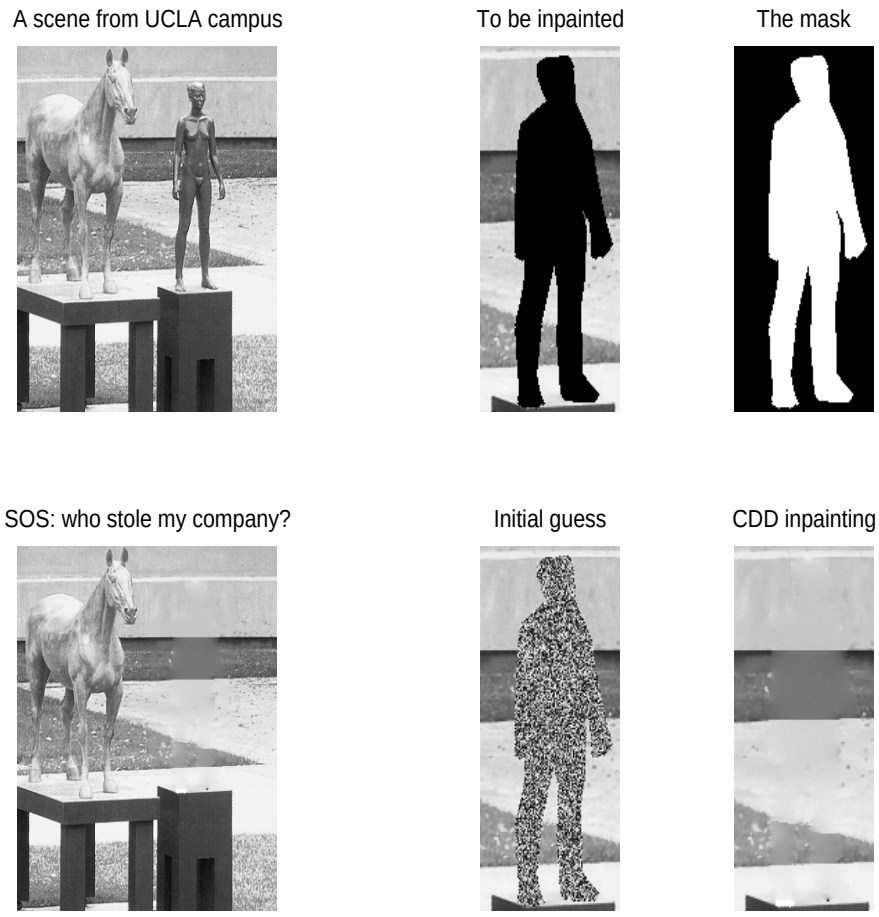

Figure 9: *"Who stole my company" (from the courtyard of Rolfe Hall, UCLA campus)?* This example shows the difficulty of real inpainting problems due to the rapid variations of isophotes and the roughness of image functions. It also illustrates why PDE based inpainting methods are not ideal for directly inpainting textures like grass in the current image. (Similar discussion can also be found in Bertalmio et al. [3].) Designing direct inpainting schemes for textures is another important task. Recent works (based on non-PDE methods) can be found in Wei and Levoy [18], and Igehy and Pereita [8].